Tweed, F. S., Roberts, M. J., and Russell, A. J., 2005. Hydrologic monitoring of supercooled discharge from Icelandic glaciers. *Quaternary Science Reviews*, **24**, 2308–2318.
Waller, R. I., 2001. The influence of basal processes on the dynamic behaviour of cold-based glaciers. *Quaternary International*, **86**, 117–128.
Wolff, E. W., Mulvaney, R., and Oates, K., 1988. The location of impurities in Antarctic ice. *Annals of Glaciology*, **11**, 194–197.

Cross-references

Anchor Ice
Cold-Based Glaciers
Creep
Formation and Deformation of Basal Ice
Frazil
Glaciohydraulic Supercooling
Rime Ice

SUPRA-GLACIAL DEBRIS ENTRAINMENTS

D. P. Dobhal
Wadia Institute of Himalayan Geology, Dehradun, India

Supra-glacial debris entrainments is defined as an unsorted and unstratified accumulation of sediments carried by the glacier along the bed and valley sides and deposited directly on glacier surface. They may occur by regelation or by the ice simply picking up the debris.

SURFACE ENERGY BALANCE

Michiel Van den Broeke[1], Xavier Fettweis[1,2], Thomas Mölg[3]
[1]Institute for Marine and Atmospheric Research, Utrecht University, Utrecht, Netherlands
[2]Department of Geography, University of Liège, Liège, Belgium
[3]Center for Climate & Cryosphere, University of Innsbruck, Innsbruck, Austria

Definition

The surface energy balance (SEB) describes the partitioning of energy fluxes toward and away from the surface. The local SEB determines the surface temperature of the Earth (T_s) and the associated exchange of energy between the surface and the atmosphere on one hand, and between the surface and the subsurface layers (whether it be soil, rock, water, snow, or ice, see Figure 1) on the other. When the surface consists of snow or ice, the SEB also determines the amount of energy that is available for sublimation and melting/freezing. These processes directly couple the SEB to the *surface mass balance* (SMB). In this entry, we describe the components of the SEB, and give six examples of the annual SEB cycle, all with a permanently snow-/ice-covered surface, but in widely varying geographical settings.

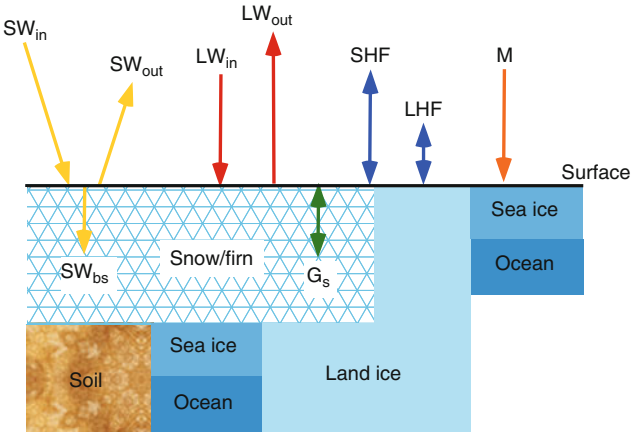

Surface Energy Balance, Figure 1 Components of the surface energy balance of snow, sea ice, and land ice. Length of arrows is only indicative.

Components of the surface energy balance

The SEB is defined as the sum of all fluxes of energy passing each second through a horizontal surface of unit area (Figure 1), with units J s^{-1} m^{-2} or W m^{-2}. *We define fluxes as positive when they are directed toward the surface,* i.e., *when they represent an energy gain for the surface.* For an infinitesimally thin surface layer without heat capacity (sometimes called a *skin layer*), these fluxes *balance,* i.e., their sum equals zero. If we neglect the heat added to the surface by falling snow, rain, or fog droplets, the SEB over a snow/ice surface can be written as:

$$M = SW_{in} + SW_{out} + SW_{bs} + LW_{in} + LW_{out} + SHF + LHF + G_s \left[Wm^{-2}\right] \quad (1)$$

In Equation 1, M is the melting flux when T_s equals 273.15 K, otherwise M = 0. Note that the melting temperature for sea ice surfaces can be lower than 273.15 K because the ice is saline in most cases. If $T_s < 273.15$ K and if there is liquid water available at the surface, M represents the freezing flux.

The abbreviations SW_{in} and SW_{out} represent the incoming and outgoing fluxes of shortwave (solar) radiation, SW_{bs} is the amount of shortwave radiation that is absorbed below the surface. LW_{in} and LW_{out} are the incoming and outgoing fluxes of longwave (terrestrial) radiation. Shortwave and longwave radiation are distinguished on the basis of their wavelength domain, determined from Planck's law by the temperature of the body that emits the radiation. If radiation originates from the surface of the Sun ($T_s \approx 5{,}800$ K), either directly or scattered in the Earth's atmosphere, nearly all energy is confined to wavelengths below 3 μm, hence the name *shortwave radiation*. If the radiation originates from the Earth-atmosphere system ($T_s \approx 200$–300 K), nearly all energy derives from wavelengths greater than 3 μm, hence the name *longwave*

radiation. SW and LW radiation fluxes are measured directly with broadband radiation sensors using selective filters.

At a sufficiently small distance above the surface, in the order of one to several mm, sensible heat exchange (SHF) and latent heat exchange (LHF) between the surface and air occurs predominantly by molecular conduction. Higher in the atmosphere, turbulence occurs as eddies (whirls) that vertically mix momentum, heat, and moisture. Turbulence is more effective in transporting scalars than molecular diffusion (Stull, 1988), and SHF and LHF are dominated by turbulent exchange. That is why they are usually referred to as *turbulent fluxes.*

Finally, G_s is the vertical heat flux below the surface, an expression of the molecular conduction of heat along temperature gradients in the snow/ice. The energy coming from the interior of the Earth, the geothermal heat flux, usually does not exceed 0.1 W m^{-2}, and is incorporated in G_s. The major components of the SEB are discussed separately below.

Shortwave radiation fluxes

When solar radiation impinges on the snow/ice surface, a part is absorbed at the surface, another part is reflected back to the atmosphere, and a third part penetrates to deeper layers and is absorbed below the surface. The net shortwave radiation flux (SW_{net}) is the total amount of shortwave radiation that is absorbed at or below the snow/ice surface. SW_{net} therefore equals the sum of downward (SW_{in}) and upward shortwave radiation (SW_{out}), and drives the daily and annual cycle in most SEB components.

SW_{in} is determined by (a) the amount of solar radiation impinging on the top of the atmosphere, (b) the amount of shortwave radiation that is scattered or absorbed in the atmosphere (depending notably on the cloudiness), and (c) the slope magnitude and orientation of the snow/ice surface. The instantaneous amount of solar radiation impinging on the top of the atmosphere (SW_{TOA}) depends on the solar constant, latitude, time of year, and time of day. Averaged over the year, the geographic poles receive about 40% of the insolation at the equator. But the temporal distribution of this energy is very different for different latitudes. As a rule of thumb, high-latitude (polar) regions experience a small daily cycle and a large annual cycle in SW_{TOA}, while tropical regions experience a large daily cycle and a small annual cycle in SW_{TOA} (Figure 2).

The amount of shortwave radiation that is scattered or absorbed in the atmosphere depends on the optical thickness of the atmosphere, which is mainly a function of vertically integrated water vapor mass and liquid water mass (clouds). The vertically integrated aerosol content also is important for shortwave radiation scattering. In the Polar Regions and for highly elevated tropical glaciers, the water vapor and aerosol content of the atmosphere is relatively low, so that the optical thickness is relatively small and the shortwave radiation intensity at the surface high. Explosive volcanic eruptions reduce the amount of solar energy reaching the surface; the El Chichón and Mount Pinatubo eruptions in 1983 and 1991 significantly impacted the SEB of Greenland (Fettweis, 2007). Glaciers or ice caps that are situated in temperate climates usually experience more cloudy conditions, limiting the amount of shortwave radiation that reaches the surface.

The orientation of glaciers with respect to the sun influences the amount of shortwave radiation impinging on the surface. If a glacier surface is steeply sloping and directed toward the sun, this can greatly enhance the amount of

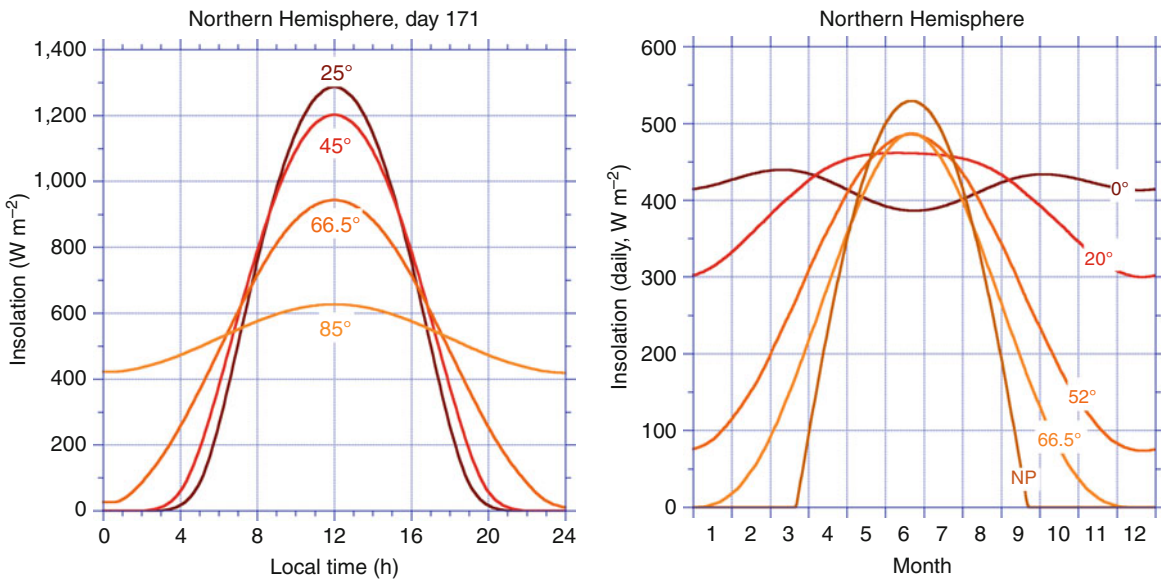

Surface Energy Balance, Figure 2 SW_{in} at the top of the atmosphere. Daily cycle in the northern hemisphere for June 20th (*left*) and annual cycle for the northern hemisphere based on daily means (*right*) of SW_{TOA} for various latitudes.

absorbed solar radiation and hence melting. On the other hand, if the sloping glacier is directed away from the sun, the solar rays hit the surface at an oblique angle, thereby decreasing the amount of shortwave radiation reaching the surface. Moreover, the surface can be shaded for parts of the day, eliminating the direct component of SW_{in}. For glacier melt modeling, the orientation of the glacier surface and the surrounding topography, therefore, needs to be explicitly taken into account (Klok and Oerlemans, 2002).

Part of the absorption (SW_{bs}) takes place below the surface (Grenfell and Maykut, 1977). Typical penetration depths are several cm in fine, dry-grained snow to several decimeters in ice (Brandt and Warren, 1993). This results in heating of the subsurface snow and ice layers (Kuipers Munneke and others, 2009) and may lead to subsurface melting (Van den Broeke and others, 2008b). When calculating the penetration of shortwave radiation in ice/snow, it is essential that the wavelength dependence of shortwave radiation absorption is taken into account, instead of using a bulk-extinction coefficient.

The fraction of shortwave radiation that is absorbed at or below the surface, is determined by the broadband surface albedo α, defined as:

$$\alpha = |SW_{out}|/SW_{in} \quad (2)$$

Snow albedo depends on the thickness, aerial coverage, and physical characteristics of the snow (grainsize, wetness, temperature), the thickness of the snow layer over dark soil and the spectrum and direction of the impinging solar radiation (wavelength distribution, solar zenith angle, ratio of diffuse to direct radiation, see Wiscombe and Warren, 1980, and entry on snow albedo). Clean, dry ice has an albedo of approximately 0.55, while clean, fresh snow has an albedo $\sim$0.85. The albedo of water ($<$0.1) is much lower than that of snow and ice, and meltwater that accumulates at the snow/ice surface can therefore have a significant impact on its albedo (Greuell, 2000).

Melting leads to rapid growth of snow grains and can lower the snow albedo to values near 0.75, i.e., increasing the amount of absorbed shortwave radiation by $\sim$70% compared to fresh snow. This represents the all-important albedo-melt feedback: melting lowers the albedo, which further enhances melt, etc. Typical low-ranging values of albedo (0.15–0.4) are found over ice and snow with a large dust load. The dust could have been melted out from the ice or blown onto it from the ice-free surroundings (Oerlemans and others, 2009). When seasonal snow or sea ice is replaced by the darker soil or sea surface, the amount of absorbed solar radiation may increase severalfold.

Figure 3 shows the global distribution of annual mean surface albedo, as derived from satellite measurements and radiative transfer modeling. The impact of snow and ice at high latitudes is clearly visible. The highest values ($>$0.8) are found over the interior dry snow zones of Greenland and Antarctica. The Arctic sea ice cover has a lower albedo, because it is melting for part of the year. The gradual transition toward lower values at mid-latitudes takes place over areas that are covered by seasonal snow or sea ice for part of the year. In the entry on snow albedo, the annual cycle of the albedo of Arctic sea ice is presented.

Longwave radiation fluxes

The net longwave radiation flux (LW_{net}) is the sum of incoming (LW_{in}) and outgoing (LW_{out}) longwave radiation fluxes. Over Greenland, LW_{in} appears the most sensitive SEB component for increased atmospheric concentrations of Greenhouse gases (Fettweis, 2007). Apart from exceptional cases, LW_{net} represents an energy loss for the surface, as the surface is generally warmer and has higher emissivity than the overlying atmosphere.

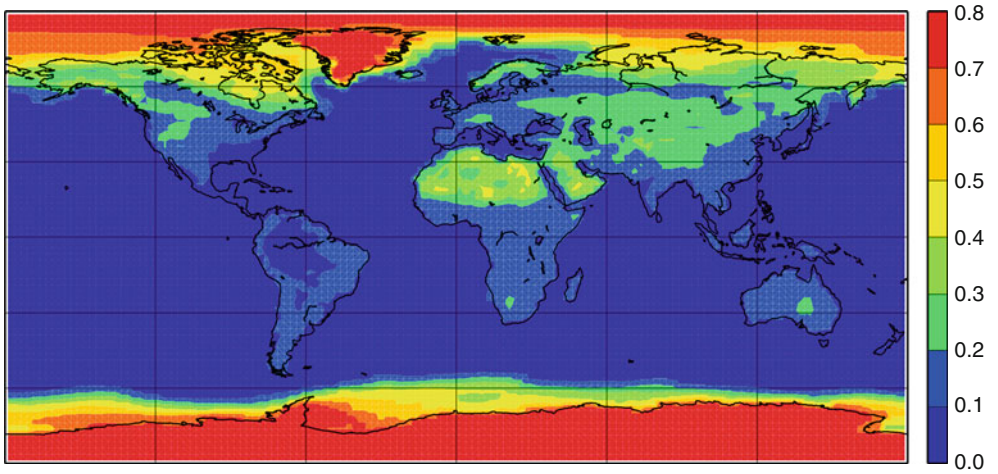

Surface Energy Balance, Figure 3 Satellite-derived surface broadband albedo, annual mean (based on data of Hatzianastassiou and others, 2004).

LW_{in} is determined by the effective emissivity (ε_{eff}) and effective radiation temperature (T_{eff}) of the atmosphere, while LW_{out} is determined by the emissivity (ε_s) and temperature (T_s) of the snow/ice surface. Using the Stephan–Boltzmann law, LW_{net} can be approximated by:

$$LW_{net} = \varepsilon_s \varepsilon_{eff} \sigma T_{eff}^4 - \varepsilon_s \sigma T_s^4 \quad (3)$$

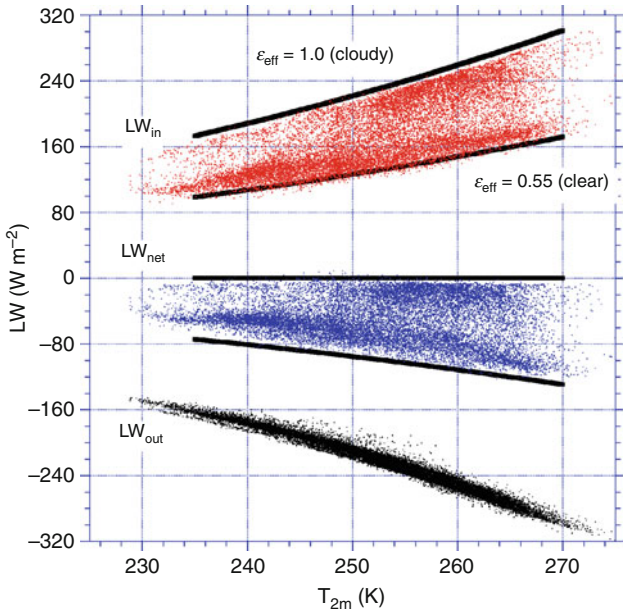

Surface Energy Balance, Figure 4 Observed hourly mean values of LW_{in} (*red dots*), LW_{out} (*black dots*), and LW_{net} (*blue dots*) as well as calculated from empirical formula (black lines, Equation 3) as a function of 2 m temperature for a non-melting location in Antarctica, at 1,100 m a.s.l. The upper and lower bounds of all three cases are for cloudy and clear sky conditions, respectively.

where the Stefan–Boltzmann constant $\sigma = 5.67 \times 10^{-8}$ W m^{-2} K^{-4}.

The surface emissivity of a dry snow surface is close to unity ($\varepsilon_s \approx 0.98$, Wiscombe and Warren, 1980) while the effective emissivity and radiation temperature of the atmosphere are complex functions of the vertical distribution of temperature, moisture, and other atmospheric compounds. In spite of this complexity, some general statements can be made. Under cloudy conditions, $\varepsilon_{eff} \approx 1$, and T_{eff} represents the cloud base temperature. When the cloud base is situated at low elevation, T_{eff} will not deviate much from T_s, so that LW_{net} will be zero or weakly negative. Under clear sky conditions, if 2 m air temperature is used as a measure for effective atmospheric radiative temperature, it is found that ε_{eff} can be approximated by a constant, to be determined empirically. Figure 4 shows an example for a location in Antarctica, where $\varepsilon_{eff} \approx 0.55$ (thick black lines in Figure 4). The resulting expression can be used to estimate LW_{in} and, if T_s is known (or assumed approximately equal to T_{2m}), to estimate LW_{out} and hence LW_{net}. The challenge lies in estimating LW_{in} for partly cloudy conditions, i.e., to interpolate between these two extremes (Kuipers Munneke and others, 2010).

Net radiation flux

Averaged over the year, $R_{net} = SW_{net} + LW_{net}$ is negative over much of the Polar Regions and in some highly elevated plateaus away from the Poles (e.g., the Tibetan Plateau, Figure 5). At these locations, cooling by LW_{net} exceeds warming by SW_{net}. This is remarkable, given that the Sun provides radiative energy for half of the time. The radiation deficit in the Polar Regions can be explained by factors that limit SW_{net}, such as the low Sun angle and the high albedo of the surface that usually consists of snow, glaciers, and sea ice. On the other hand, the snow effectively emits longwave radiation ($\varepsilon_s \approx 1$) while the polar

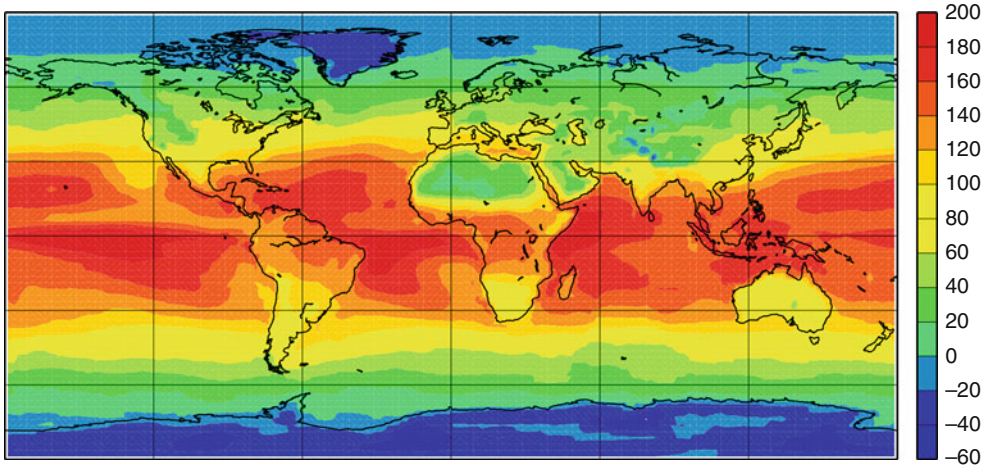

Surface Energy Balance, Figure 5 Annual average surface net radiation in W m^{-2} (*based on data of* Hatzianastassiou and others, 2004).

atmosphere is cold and dry, resulting in small ε_{eff}. This results in relatively strongly negative values of LW_{net}. Even at these sites, R_{net} will become positive around noon during sunny summer days, but when averaged over the year, the radiation balance is negative. Over a semi-infinite snow pack, this radiation deficit must be compensated by the sensible heat flux from the atmosphere, as the heat flux from the snowpack equals approximately zero when averaged over the year (see Section Subsurface heat flux). The latent heat flux is also likely to be small at polar sites (see Section latent heat flux), so that the most likely candidate is a flux of sensible heat from the atmosphere to the surface (next Section "Sensible heat flux"). Over sea ice, heat provided by the ocean through the subsurface heat flux compensates an important part of the radiative heat loss. Over open water in winter, much of the radiative heat loss is invested in cooling the upper ocean layers, resulting in the formation of sea ice.

Sensible heat flux

The turbulent flux of sensible heat, SHF (often referred to as the sensible heat flux), describes heat exchange between the surface and the air above it. In the surface layer, SHF can be directly measured using sonic anemometers that measure rapid (turbulent) fluctuations in temperature and vertical velocity. But these instruments are relatively vulnerable and expensive, which is why the sensible heat flux is often calculated, based on measured profiles of wind and temperature, in combination with surface-layer similarity theory (Stull, 1988). These calculations usually give satisfactory results over melting and non-melting snow and ice surfaces.

The sensible heat flux is directed away from the surface (negative) when the surface is warmer than the air, i.e., under statically unstable conditions in the atmospheric surface layer (SL). This upward heat transport is often referred to as convection. In the Polar Regions, convection is rare, and occurs, for instance, when cold polar air flows over open water, forming characteristic convective cloud straits. Weak convection also occurs during summer at highly elevated sites on the Polar Ice sheets, where temperatures are too low for sublimation to be significant (King and others, 2006).

In general, however, the negative net radiation cools the surface, which then becomes colder than the air above. Therefore, over snow and ice, SHF is commonly positive, i.e., directed toward the surface. The associated cooling of the atmospheric boundary layer often results in a surface-based temperature inversion, in which the temperature increases with height. In regions where the radiative heat loss is quasi-permanent during the Polar Night, i.e., the elevated interior plateaus of the Greenland and Antarctic ice sheets, the surface temperature inversion can become several tens of degrees (e.g., Vostok station in Figure 6). In the coastal areas and in the Arctic (Overland and others, 2000), the radiative cooling is weaker because of the more frequent occurrence of clouds, enhancing incoming

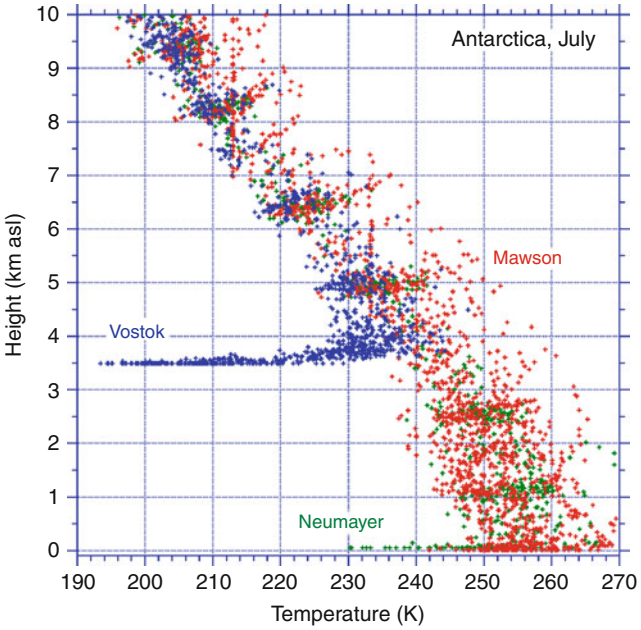

Surface Energy Balance, Figure 6 Wintertime (July) vertical temperature profiles from radiosondes measurements at three Antarctic stations. Atmospheric temperature profiles at South Pole are similar to Vostok.

longwave radiation, resulting in a weaker surface temperature inversion (e.g., Mawson and Neumayer in Figure 6).

Under these statically stable conditions, wind shear is a prerequisite for the generation of turbulent heat exchange. Wind shear is enhanced over rough surfaces, such as hummocky sea ice (Andreas and Claffey, 1995); over snow and ice surfaces that are relatively smooth, it requires relatively large wind speeds for the wind shear to become sufficiently large. Over ice sheets and glaciers, which have a sloping surface, this wind shear is often provided by *katabatic* forcing. The cold near-surface air is denser than the air in the free atmosphere at the same elevation, which sets up a horizontal pressure gradient over a sloping surface, forcing *katabatic* or downslope winds. Over the large ice sheets, katabatic winds can be very persistent. Because the katabatic forcing acts along the local slope, katabatic winds have a high *directional constancy.* Because of their direct coupling to the radiative cooling of the surface, katabatic winds efficiently generate the turbulence necessary to keep the sensible heat transport going in the stably stratified atmospheric surface layer.

Latent heat flux

Over a snow/ice surface at freezing temperatures, the latent heat flux (LHF) equals the amount of heat extracted from or added to the surface as a result of sublimation (the phase change from solid to water vapor) or deposition (phase transition from vapor to solid, i.e., rime formation). When the surface is melting and liquid water is available, LHF equals the amount of heat extracted from or added to

the surface as a result of evaporation (the phase change from liquid to gas) or condensation (phase transition from gas to liquid, i.e., dew formation). In mountainous areas and over sea ice, frost formation (from liquid to solid) may also be an important process. All these processes exchange not only heat but also mass with the surface, which couples the surface energy balance to the surface mass balance (the sum of all mass fluxes toward and away from the surface).

The LHF can be directly measured using instruments that measure the absorption of light by water vapor at a specific wavelength. Alternatively, LHF can be calculated using simultaneously measured vertical profiles of wind speed and specific humidity. The latter is often determined from relative humidity measurements, which are difficult to perform over snow and ice (Anderson, 1994).

Temperature plays a pivotal role in the magnitude of LHF through its influence on the moisture content of the air. The maximum moisture content of the air, and therewith its vertical gradients, is tightly coupled to temperature through the Clausius Clapeyron equation. Figure 7 (left) shows specific humidity as a function of 2 m temperature for a non-melting location in East Antarctica. Neglecting the temperature difference between the surface and 2 m for the moment and using the fact that the snow/ice surface is always saturated (i.e., the surface-specific humidity is represented by the upper boundary of the point cloud), the distance of individual points to the upper boundary represents the vertical moisture gradient, and therewith the sublimation potential. The undersaturation and therewith the vertical humidity gradient become small at low temperatures, resulting in low LHF values (Figure 7, right).

In summer, when the surface absorbs solar radiation and heats up, significant sublimation does occur at this site (significantly negative LHF). But even under very favorable conditions, the magnitude of LHF usually does not exceed several tens of W m^{-2}, which are small values compared to the mid-latitudes and tropics, where LHF can attain values of several hundreds of W m^{-2}. But this does not mean that LHF is unimportant for the hydrological cycle at high latitudes. An average LHF of only -1 W m^{-2} still represents a surface mass loss of 11 kg m^{-2}. For areas where snowfall and melt are small, such as the interior of the Greenland and Antarctic ice sheets, this potentially represents a considerable fraction of the annual snowfall.

When snowdrift takes place, sublimation from the surface ceases while the sublimation of drifting snow particles takes over. For snowdrift sublimation, which is thought to be an important term in the mass balance of the Greenland and Antarctic ice sheets and the seasonal snowpack at high northern latitudes (Box and others, 2006; Déry and Yau, 2001), no robust measurement techniques are yet available.

Subsurface heat flux

The subsurface heat flux (G) represents the conduction of heat into the subsurface strata; this flux is mainly driven by molecular conduction and therefore occurs along vertical temperature gradients in the snow/ice, following $G(z) = k\, dT(z)/dz$. The heat conductivity (k) of snow is mainly a function of snow density and grain structure, connecting the low heat conductivity of air ("zero" density snow) to that of ice (red curve in Figure 8). Since snow is

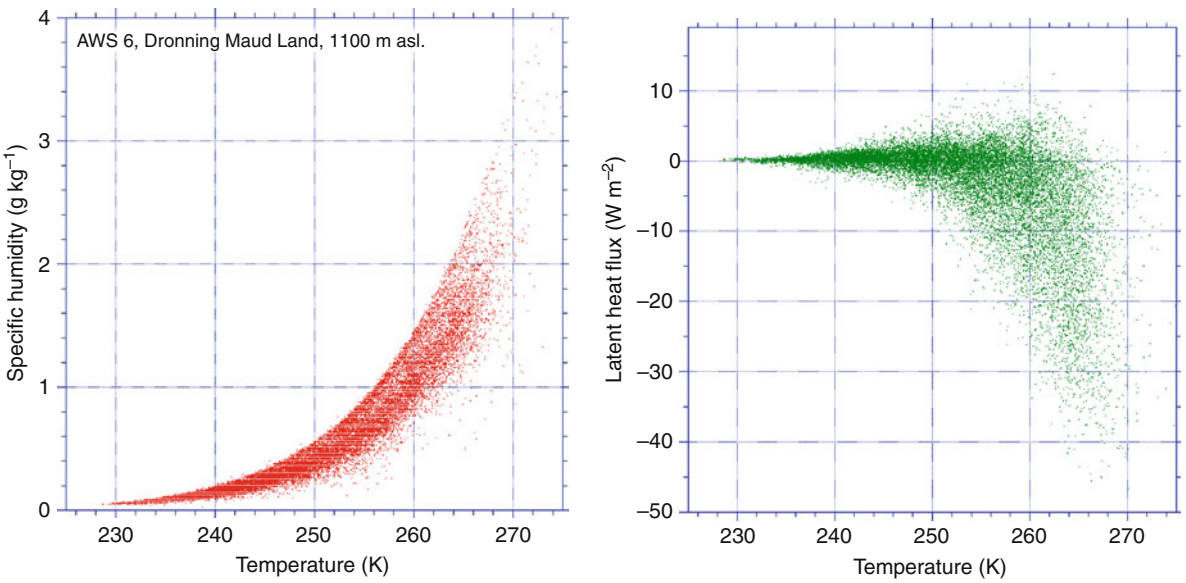

Surface Energy Balance, Figure 7 Observations of hourly 2 m specific humidity (*left*) and calculated latent heat flux LHF (*right*) as a function of 2 m temperature at an automatic weather station in East Antarctica.

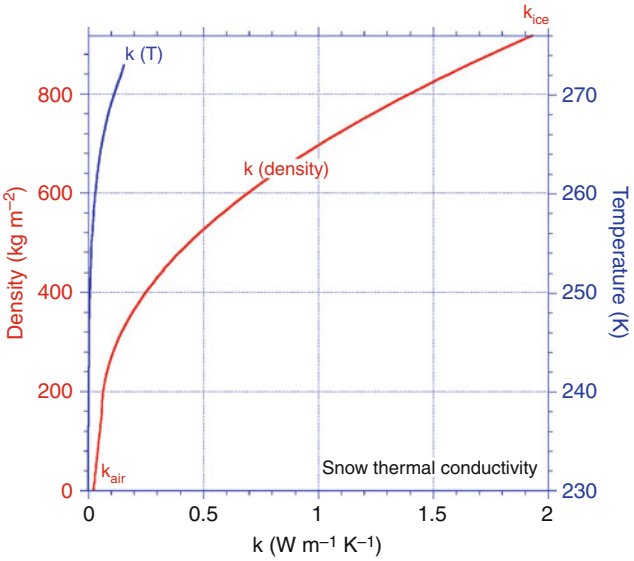

Surface Energy Balance, Figure 8 Value of heat conductivity k in snow is mainly a function of snow density and grain structure (*red curve*). A small part of the heat transport results from internal convection and from sublimation and subsequent deposition elsewhere in the snowpack, mainly a function of temperature (*blue curve*).

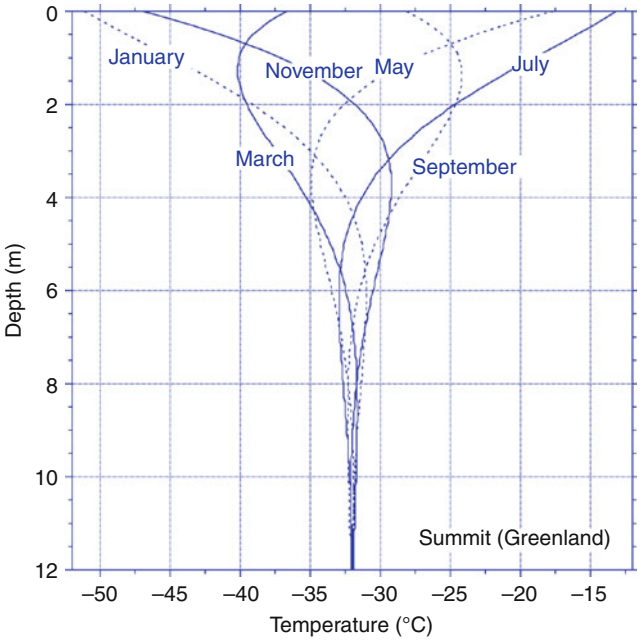

Surface Energy Balance, Figure 9 Theoretical temperature distribution in the snow at Summit, Greenland, forced by a sinusoidal temperature variation at the surface, and assuming a homogeneous snowpack with k = 0.5 W K^{-1} m^{-1}.

a porous medium, a small part of the heat transport results from internal convection and from sublimation and subsequent deposition elsewhere in the snowpack, both processes being a function of temperature (blue curve in Figure 8). This results in an effective heat conductivity that is the sum of conduction and internal convection/deposition.

In the surface energy balance, the surface value of G, G_s, is relevant. Over sea ice, G_s is an important SEB component (see further in this entry). Over a semi-infinite snowpack, G_s will be close to zero when averaged over the year; otherwise the snow layers below the surface would continuously cool or heat up. In the monthly average, G_s will be negative in summer, when the surface is warmer than the subsurface snow layers and heat is transported into the snowpack, and positive in winter, when the temperature gradient is reversed and heat is extracted from the deeper snow layers. But also monthly average values are usually small, typically several W m^{-2}. The real importance of G_s is in the daily cycle of the SEB. At times when turbulence is small, for instance under weak wind conditions, G_s is the only term that can compensate the radiative heat gains/losses; the chain of events is as follows: when the radiation balance becomes strongly positive/negative, and turbulence is weak, the surface temperature will quickly rise/fall. In response, the vertical temperature gradients between the subsurface and the surface will quickly grow, triggering a strongly negative/positive value of G_s, which compensates for the radiative heat exchange.

Because it transports heat, G(z) determines the ice/snow temperature distribution. Figure 9 shows the (theoretical) subsurface temperature distribution at Summit Station at the top of the Greenland ice sheet, as forced by a sinusoidal annual cycle in surface temperature, assuming a homogenous snowpack with constant density. In the absence of melting, the annual temperature variation vanishes below approximately 10 m depth. This means that at those depths, the temperature approximates the annual mean surface temperature. This technique is often used to estimate the annual mean surface temperature in the interior of the large ice sheets, where few observations are available. When melt occurs, the refreezing of the percolating meltwater releases heat into the snowpack and the underlying ice. Under these conditions, the technique of determining annual mean T_s is no longer applicable.

Melting and refreezing

If absorption of solar radiation has heated the snow/ice layers to the melting point, the excess energy produces melting ($M > 0$). The meltwater formed at the surface either runs off (when the surface is impermeable, i.e., ice), or penetrates the snowpack. Sea ice is an intermediate case where the water partly pools at the surface and partly percolates through or flows off the ice into the ocean. In the case of a snow pack, the meltwater may refreeze at some depth where the temperature is still below freezing. This refreezing of meltwater may constitute an important process for the mass balance of glaciers and sea ice

because the ice involved must be melted more than once before it is removed from the glacier. Moreover, upon refreezing, latent heat is released within the snowpack, which alters the subsurface temperature distribution. However, because the heat is released below the surface, as is the case with penetration of shortwave radiation, this heat source is not part of the surface energy balance. It merely influences the SEB through altering the subsurface heat flux by changing the subsurface temperature gradient. Gallée and Duynkerke (1997), for instance, showed that the daily cycle of surface melting and refreezing below the surface significantly impacts the SEB in Greenland. If it is not taken into account, the surface and subsurface temperatures are significantly underestimated.

Annual cycle of SEB over various permanent snow- and ice-covered surfaces

In this section, we discuss the idealized annual cycle, based on monthly means, of the SEB over various permanently snow- and ice-covered surfaces. The coordinates, elevation, surface type and basic climate conditions of these locations during different seasons are summarized in Table 1. For clarity, the annual cycles presented in the following figures have been smoothed using 3-month running means. For details of calculation and variability beyond the mean annual cycle, we refer to the original references.

North pole, arctic basin

While some SEB estimates are available from Russian drifting station and from various US drift stations such as SHEBA (Surface Heat Budget of the Arctic Ocean, Utta and others, 2002; Persson and others, 2002), here we present, for illustrative purposes, the idealized annual cycle of the SEB at the North Pole (90° North, NP), based on model/weather observations combined with an SEB model, assuming 2 m thick sea ice. The NP is situated over a frozen ocean surface that consists of snow-covered sea ice in winter and melting snow/ice in summer (Table 1). The wintertime SEB (Figure 10) is a first-order balance between (longwave) radiative cooling and heating by SHF and G_s. Especially G_s is significant; 30 W m^{-2} is the approximate amount of heat that flows from the warm ocean (−1.8°C) to the sea ice surface (−30°C), when the ice is 2 m thick. Because of the radiative cooling, the sea ice surface is colder than the overlying air, which, in combination with the moderate winds, generates a flux of sensible heat toward the surface. At the sea ice–ocean boundary, a semi-unlimited heat source is available from the deeper ocean. As a result, annual average G_s is significantly positive, driving freezing at the ice/ocean interface.

At these low temperatures, wintertime LHF is negligible. In spring, shortwave radiative heating increases surface temperature and specific humidity, resulting in weak sublimation. At sea level, the summer climate is relatively mild, even this far north, and frequent melting occurs. When melting starts in earnest in summer, the moisture and temperature gradients between the sea ice surface and the overlying air diminish, reducing the magnitude of the turbulent fluxes. Because the temperature gradient between ice surface and ice base also disappears, G_s goes to zero. All the absorbed shortwave radiation is invested in melting. The integrated amount of melt energy represents the removal of approximately 1.5 m of ice, less than the total ice thickness. In spite of bottom melting also taking place, sea ice at the North Pole usually survives the summer melt period, to form multiyear sea ice in the subsequent years.

Ablation zone of the west-greenland ice sheet

The Greenland ice sheet is the second largest ice mass in the world, and its southernmost part is situated in a subarctic climate. A site was selected in the lower ablation zone of the southwestern ice sheet (Table 1) for which reliable, multiyear meteorological observations are available (Van den Broeke et al., 2008a, b). In winter, surface radiative cooling is compensated in first order by SHF, with small contributions from LHF and G_s (Figure 11).

Surface Energy Balance, Table 1 Surface and climate characteristics of some SEB locations

Location name	Coordinates Elevation (m asl)	Surface type		Temperature (°C)		Wind speed (m s^{-1})	
		Summer	*Winter*	*Summer*	*Winter*	*Summer*	*Winter*
North Pole (Sea Ice)	90° N ~0 m	Melting snow/ice	Snow	−2	−30	6	5
West Greenland ablation zone	67° 06′N, 50° 07′ W 500 m	Melting ice	Snow	+3	−20	5	5
Morteratsch glacier	46° 24′ N, 9° 56′ E 2100 m	Melting ice	Snow	+9	−7	6	6
Neumayer (Antarctica)	70° 39′ S, 8° 15′ W 40 m	(Melting) snow	Snow	−5	−25	7	10
South Pole (Antarctica)	90° S 2830 m	Snow	Snow	−30	−60	5	7
		Dry season	*Wet season*	*Dry season*	*Wet season*	*Dry season*	*Wet season*
Kersten glacier (Kilimanjaro)	3° 05′ S, 37° 21′ E 5873 m	Ice	(Melting) snow	−7	−6	4	5

The subsurface heat flux G_s is heating the surface during winter, when the surface temperature is lower than the deeper snowpack temperature (Figure 9). In summer, the surface at this site is continuously at the melting point while the temperature deeper in the snowpack is several degrees lower than the melting point inducing a negative G_s.

Because in summer the air is usually warmer than 0°C, both SHF and LHF are directed toward the melting ice surface, contributing significantly to melt. Because of the sunny climate and relatively high temperatures in this part of Greenland, the total amount of summer ice melt at this site exceeds 4 m, among the largest values found in Greenland. Both SHF and LHF show a double maximum, one in winter and one in summer, which is caused by the double maximum in wind speed. In both seasons, atmospheric cooling through SHF maintains the katabatic winds. In winter, surface radiative cooling maintains the surface temperature deficit, while in summer the melting surface is responsible for a temperature deficit. Over melting ice surfaces, katabatic winds are sometimes called *glacier winds*.

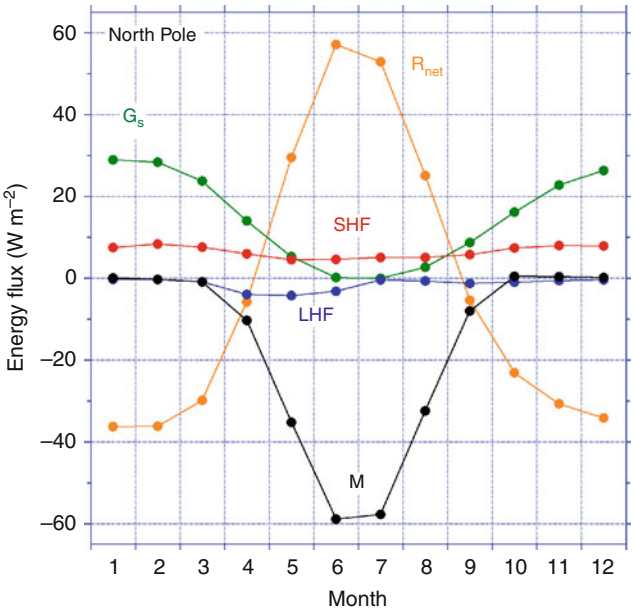

Surface Energy Balance, Figure 10 Annual cycle of SEB components at North Pole in the Arctic basin. Idealized results from model data and observations, assuming 2 m thick sea ice (see text).

Ablation zone of morteratsch glacier, swiss alps

Vadret da Morteratsch is a mid-latitude glacier in Switzerland (Table 1) and has one of the longest uninterrupted SEB records from the surface of a valley glacier (15 years, Oerlemans and others, 2009). The automatic weather station that produced the results shown in Figure 12 is situated in the ablation zone at the tongue of the glacier at 2,100 m asl. The winter SEB (Figure 12) is comparable to the Greenland ablation zone, with radiative heat losses being compensated mainly by SHF. In summer, the glacier tongue is surrounded by ice-free terrain, resulting in high summer air temperatures over the melting ice surface

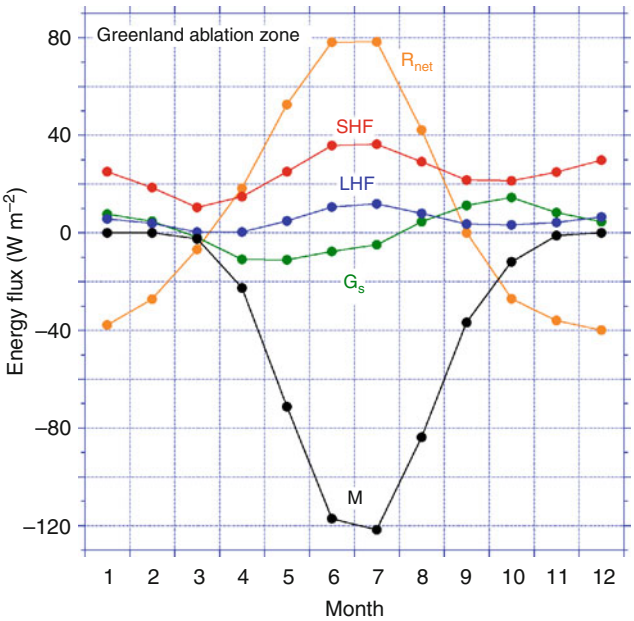

Surface Energy Balance, Figure 11 Annual cycle of SEB components in the lower ablation zone of the ice sheet in southwest Greenland. SEB calculated from 4 years of automatic weather station observations (see text).

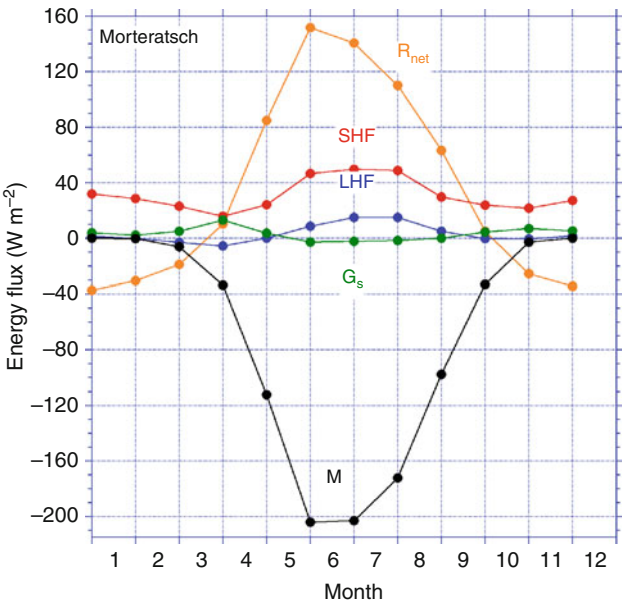

Surface Energy Balance, Figure 12 Annual cycle of SEB components in the ablation zone of the Morteratsch glacier, Switzerland. SEB calculated from 15 years of automatic weather station observations (see text).

(Table 1). This also results in dust accumulation, so that the surface albedo of the ice attains very low values (~0.15). This strongly enhances the absorption of shortwave radiation and therewith surface melting. As a result, R_{net} attains much higher values than in Greenland, while SHF and LHF are comparable, including the double annual maxima. The total melt for this location exceeds 7 m of ice, which has forced a strong retreat of the glacier in recent decades.

Kersten glacier, Kilimanjaro

This tropical glacier is situated between 5,100 and 5,900 m on the southern flank of Kilimanjaro, close to the equator (Table 1). Based on several years of AWS data and distributed energy balance modeling, the SEB, averaged over the entire glacier surface, could be determined (Mölg and others, 2009). The annual cycle (Figure 13) deviates strongly from other locations. As a result of its location close to the equator, the annual cycles in SW_{in} and ambient temperature are small, and thus there is no climatological summer or winter at this site; the seasonal variations are mostly forced by the wet and dry seasons. At these high elevations, the air contains little moisture and sublimation produces an important heat and mass loss year round. In the main wet season (April/May), sublimation strongly decreases. Net radiation is small, because SW_{net} is at a minimum, mainly due to high albedo. At the same time, as the air is moist and cloudy, cooling by LW_{net} is also small, resulting in small net radiation. In the core dry season (June–August) there is hardly any melt and ablation is controlled by sublimation. In these months, cooling by sublimation significantly exceeds warming by R_{net}, so that the surface remains significantly colder than the overlying air and SHF peaks. The most variable part of the year is the wet season around November/December. This season can start in October and last into January/February, but sometimes is totally absent. The occurrence of sublimation and the associated surface cooling is vital for limiting the melt amount throughout the year. Note that, even in the presence of moderate refreezing, melt (575 kg m^{-2} $year^{-1}$) still removes more mass than sublimation (450 kg m^{-2} $year^{-1}$) glacier-wide, because of the much smaller latent heat of fusion compared to evaporation/sublimation. However, at the glacier summit, sublimation dominates and accounts for 75% of the total annual mass loss.

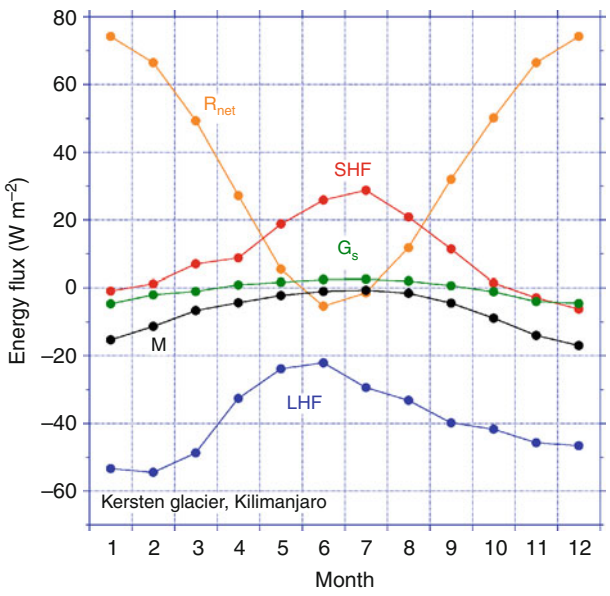

Surface Energy Balance, Figure 13 Annual cycle of SEB components on Kersten glacier, Kilimanjaro, Tanzania. SEB calculated from three years of automatic weather station observations in combination with a distributed energy balance model (see text).

Neumayer, antarctica

Neumayer station (Germany) is situated on Ekstrøm ice shelf in coastal East Antarctica, at approximately 70°S (Table 1). The station is situated relatively far to the north, at low elevation (40 m asl) and close to the Southern Ocean. The nearby ocean is ice-covered in winter, but ice free in summer. Being situated close to the circumpolar pressure trough, Neumayer experiences strong easterly winds year round with frequent occurrence of snowdrift (~40% of the time). The wind maximum in winter is caused by enhanced depression activity, not by katabatic forcing, because Neumayer is situated on a flat ice shelf, which does not allow for significant katabatic forcing. In spite of the proximity of the ocean, Neumayer has a cold climate with only occasional melting around noon during sunny summer days. The SEB (Figure 14) was calculated using 13 years of high-quality meteorological observations (König Langlo and Loose, 2007; Van den Broeke and others, 2009). In the absence of continuous melting, with slow snow metamorphosis, the surface albedo is high year round. Only after prolonged dry periods with daytime melt in summer does the albedo of the snow surface fall below 0.8; as a result, R_{net} is small and the radiation balance only becomes positive in summer. In combination with mild summer temperatures, this allows for significant sublimation (Figure 14). In winter, longwave radiative cooling dominates and is compensated by SHF and in second order by LHF and G_s.

South pole, east antarctica

The geographic South Pole is situated in the vast interior of the East Antarctic ice sheet at an altitude in excess of 2,800 m (Table 1). The South Pole experiences a wintertime surface inversion similar to Vostok Station in Figure 6. Because it is not situated on a dome, the wind climate shows an appreciable wintertime (katabatic) maximum which, because the surface slope is small, is much weaker than those measured over the steeper parts of the ice sheet closer to the coast. Snow metamorphism is slow at these low temperatures, resulting in a year-round high surface albedo. As a result, summertime net radiation is

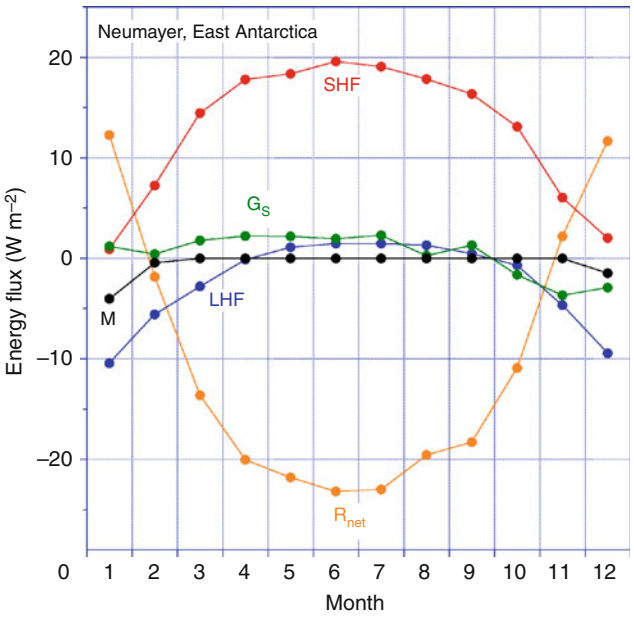

Surface Energy Balance, Figure 14 Annual cycle of SEB components at Neumayer, East Antarctica. SEB calculated based on 13 years of surface observations (see text).

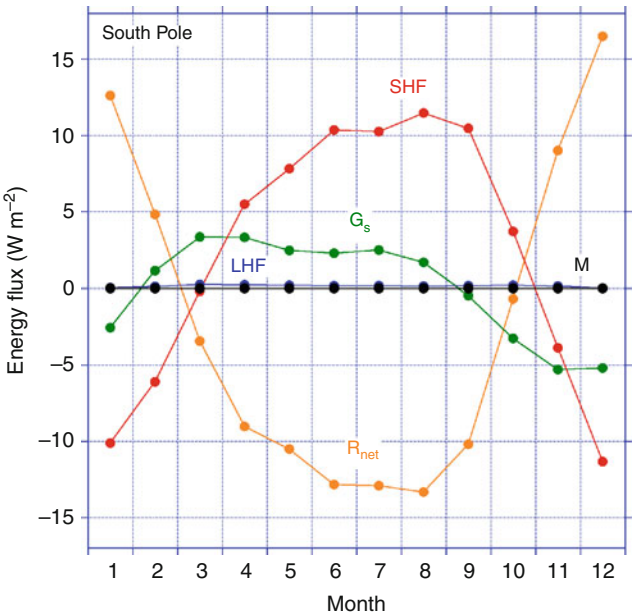

Surface Energy Balance, Figure 15 Annual cycle of SEB components at South Pole, East Antarctica. SEB calculated based on 3 years of surface observations (see text).

small, <15 W m^{-2}, and all fluxes are smaller in magnitude than at Neumayer (Figure 15). Summer temperatures are also too low to allow for significant sublimation to occur. In the absence of this heat sink, surface temperature can rise quickly above the air temperature during sunny summer days, allowing weak convection (negative SHF) and a shallow (~100 m) mixed boundary layer to develop (King and others, 2006; Van As and others, 2006). Because all other fluxes are small, monthly mean G_s becomes a significant component of the SEB at the South Pole, in spite of its small magnitude. The wintertime SEB is comparable to Neumayer, i.e., a first-order balance between radiative cooling and heating by SHF.

Summary

This entry describes the components of the surface energy balance (SEB) over snow and ice: shortwave and longwave radiation, the turbulent fluxes of sensible and latent heat, and the subsurface (conductive) heat flux. If the surface is melting, the sum of these fluxes determines the melt rate. We explicitly describe the idealized mean annual cycle of the surface energy balance components at six locations with permanently ice- or snow-covered surfaces, but with widely varying melt characteristics: sea ice at the North Pole, the ablation zone of the Greenland ice sheet, the ablation zone of the Morteratsch glacier in Switzerland, Kersten Glacier on the Kilimanjaro in Tanzania, Neumayer station in coastal East Antarctica, and South Pole station in interior East Antarctica.

Acknowledgments

We thank Gert König Langlo, Rianne Giesen, and Hans Oerlemans for providing data. Thomas Grenfell and an anonymous reviewer are thanked for improving the original manuscript.

Bibliography

Anderson, P. S., 1994. A method for rescaling humidity sensors at temperatures well below freezing. *Journal of Atmospheric and Oceanic Technology*, **11**, 1388–1391.

Andreas, E. L., and Claffey, K. J., 1995. Air-ice drag coefficients in the western Weddell Sea: 1. Values deduced from profile measurements. *Journal of Geophysical Research*, **100**, 4821–4831.

Box, J., Bromwich, D., Veenhuis, B., Bai, L.-S., Stroeve, J., Rogers, J., Steffen, K., Haran, T., and Wang, S.-H., 2006. Greenland ice sheet surface mass balance variability (1988–2004) from calibrated polar MM5 output. *Journal of Climate*, **19**, 2783–2800.

Brandt, R. E., and Warren, S. G., 1993. Solar heating rates and temperature profiles in Antarctic snow and ice. *Journal of Glaciology*, **39**, 99–110.

Déry, S. J., and Yau, M. K., 2001. Simulation of blowing snow in the Canadian Arctic using a double-moment model. *Boundary-Layer Meteorology*, **99**, 297–316.

Fettweis, X., 2007. Reconstruction of the 1979–2006 Greenland ice sheet surface mass balance using the regional climate model MAR. *The Cryosphere*, **1**, 21–40.

Gallée, H., and Duynkerke, P., 1997. Air-snow interactions and the surface energy and mass balance over the melting zone of west Greenland during GIMEX. *Journal of Geophysical Research*, **102**, 13813–13824.

Grenfell, T. C., and Maykut, G. A., 1977. The optical properties of ice and snow in the Arctic basin. *Journal of Glaciology*, **18**, 445–463.

Greuell, W., 2000. Melt-water accumulation on the surface of the Greenland ice sheet: effect on albedo and mass balance. *Geografiska Annaler*, **82A**, 489–498.
Hatzianastassiou, N., Matsoukas, C., Hatzidimitriou, D., Pavlakis, C., Drakakis, M., and Vardavas, I., 2004. Ten year radiation budget of the Earth: 1984–93. *International Journal of Climatology*, **24**, 1785–1802.
King, J. C., and Connolley, W. M., 1997. Validation of the surface energy balance over the Antarctic ice sheets in the UK meteorological office unified climate model. *J Climate*, **10**, 1273–1287.
King, J. C., Argentini, S. A., and Anderson, P. S., 2006. Contrasts between the summertime surface energy balance and boundary layer structure at Dome C and Halley stations, Antarctica. *Journal of Geophysical Research*, **111**, D02105, doi:10.1029/2005JD006130.
Klok, E. J., and Oerlemans, J., 2002. Model study of the spatial distribution of the energy and mass balance of Morteratschgletscher, Switzerland. *Journal of Glaciology*, **48**, 505–518.
König-Langlo, G. C., and Loose, B., 2007. The meteorological observatory at Neumayer stations (GvN and NM-II). *Antarctica, Polarforschung*, **76**, 25–38.
Kuipers Munneke, P., van den Broeke, M. R., Reijmer, C. H., Helsen, M. M., Boot, W., Schneebeli, M., and Steffen, K., 2009. The role of radiation penetration in the energy budget of the snowpack at Summit, Greenland. *The Cryosphere*, **3**, 155–165.
Kuipers Munneke, P., Reijmer, C. H., and van den Broeke, M. R., 2010. Assessing the retrieval of cloud properties from radiation measurements over snow and ice. *International Journal Climatology*, doi:10.1002/joc.2114.
Mölg, T., Cullen, N. J., Hardy, D. R., Winkler, M., and Kaser, G., 2009. Quantifying climate change in the tropical mid troposphere over East Africa from glacier shrinkage on Kilimanjaro. *Journal of Climate*, **22**, 4162–4181.
Oerlemans, J., Giessen, R. H., and van den Broeke, M. R., 2009. Retreating alpine glaciers: increased melt rates due to accumulation of dust (Vadret da Morteratsch, Switzerland). *Journal of Glaciology*, **55**, 729–736.
Overland, J. E., McNutt, S. L., Groves, J., Salo, S., Andreas, E. L., and Persson, P. O. G., 2000. Regional sensible and radiative heat flux estimates for the winter Arctic during the Surface Heat Budget of the Arctic ocean (SHEBA) experiment. *Journal of Geophysical Research*, **105**, 14093–14102.
Persson, P. O. G., Fairall, C. W., Andreas, E. L., Guest, P. S., and Perovich, D. K., 2002. Measurements near the atmospheric surface flux group tower at SHEBA: near-surface conditions and surface energy budget. *Journal of Geophysical Research*, **107** (C10), 8045, doi:10.1029/2000JC000705.
Stull, R. B., 1988. *An introduction to boundary layer meteorology*. Dordrecht/Boston/London: Kluwer Academic Publishers, p. 666.
Uttal, T., Curry, J. A., McPhee, M. G., Perovich, D. K., Moritz, R. E., Maslanik, J. A., Guest, P. S., Stern, H. L., Moore, J. A., Turenne, R., Heiberg, A., Serreze, M. C., Wylie, D. P., Persson, O. G., Paulson, C. A., Halle, C., Morison, J. H., Wheeler, P. A., Makshtas, A., Welch, H., Shupe, M. D., Intrieri, J. M., Stamnes, K., Lindsey, R. W., Pinkel, R., Pegau, W. S., Stanton, T. P., and Grenfell, T. C., 2002. The surface heat budget of the Arctic. *Bulletin of the American Meteorological Society*, **83**, 255–275.
Van As, D., van den Broeke, M. R., and Helsen, M. M., 2006. Structure and dynamics of the summertime atmospheric boundary layer over the Antarctic plateau, I: measurements and model validation. *Journal of Geophysical Research*, **111**, D007102, doi:10.1029/2005JD005948.
Van den Broeke, M. R., Smeets, C. J. P. P., Ettema, J., van der Veen, C., van de Wal, R. S. W., and Oerlemans, J., 2008a. Partitioning of melt energy and meltwater fluxes in the ablation zone of the west Greenland ice sheet. *The Cryosphere*, **2**, 179–189.
Van den Broeke, M., Smeets, P., Ettema, J., and Munneke, P. K., 2008b. Surface radiation balance in the ablation zone of the west Greenland ice sheet. *Journal of Geophysical Research*, **113**, D13105, doi:10.1029/2007JD009283.
Van den Broeke, M. R., König-Langlo, G., Picard, G., Kuipers Munneke, P., and Lenaerts, J., 2009. Surface energy balance, melt and sublimation at Neumayer station, East Antarctica. *Antarctic Science*, doi:10.1017/S0954102009990538.
Wiscombe, W., and Warren, S., 1980. A model for the spectral albedo of snow I. Pure snow. *Journal of Atmospheric Sciences*, **37**, 2712–2733.

Cross-references

Albedo
Arctic Hydroclimatology
Atmosphere-Snow/Ice Interactions
Climate Change and Glaciers
Degree-Days
Dry Snow
Firn
Glacier Mass Balance
Heat and Mass Transfer in Sea Ice
Ice Sheet
Ice Shelf
Katabatic Wind: In Relation with Snow and Glaciers
Kilimanjaro
Latent Heat of Condensation
Latent Heat of Fusion/Freezing
Latent Heat of Sublimation
Melting Processes
Physical Properties of Snow
Sea Ice
Snow
Snow Density
Snow Drift
Surface Temperature of Snow and Ice
Temperature Profile of Snowpack

SURFACE TEMPERATURE OF SNOW AND ICE

Dorothy K. Hall
Crysopheric Sciences Branch, Greenbelt, MD, USA

Definition

Land-Surface Temperature (LST) – surface temperature measurement from space over land areas, including land ice and snow.

Introduction and background

Thermal infrared (TIR) sensors facilitate surface temperature and melt-condition monitoring over extensive areas of snow and ice (Key and Haefliger, 1992; Stroeve and Steffen, 1998; Comiso, 2006; Hall et al., 2006, 2008a, b), especially when used with complementary satellite-derived passive- and active-microwave data.

The surface temperature (T) is not an intrinsic property of the surface; it varies with external factors such as meteorological conditions. Emissivity *is* an intrinsic property